

THEORY OF INTERFEROMETRY AND APERTURE SYNTHESIS

ABSTRACT. The basics of interferometry are covered in these lectures. We first discuss a simple interferometer and show that the output is proportional to the Fourier transform of the sky brightness. This leads to the concept of aperture synthesis. The geometrical effects of Earth rotation, the idea of fringe frequency and the resolution or (u,v) plane are then discussed. Finally the formation of images from interferometer data is outlined. The appendix contains a description of further complicating effects which limit the field of view of practical interferometers.

1 Interferometers

1.1 Why interferometers?

A major consideration in radio astronomy is that of resolution. Early discoveries in radio astronomy were made with single telescopes with resolutions of a degree or so and it rapidly became obvious that many celestial radio sources were smaller than this in angular size. Optical observations are generally limited by atmospheric seeing to a resolution of around 1 arc sec. To achieve this resolution at wavelengths of 1 m requires telescopes of 200 km in diameter. The only practical way to achieve this is to use smaller, more practical telescopes but spaced by 100's of km and connected as an interferometer array hence the MERLIN system. We now know that there is a lot of interesting astrophysics to be investigated on scales from arcsec down to millarcsec requiring both connected element and Very Long Baseline Interferometry (VLBI) techniques. We will look at the properties of simple interferometers in the next section, then discuss geometrical effects before describing how images are formed. The appendix contains a discussion of effects which limit the field of view of an interferometer, and can be missed on a first reading.

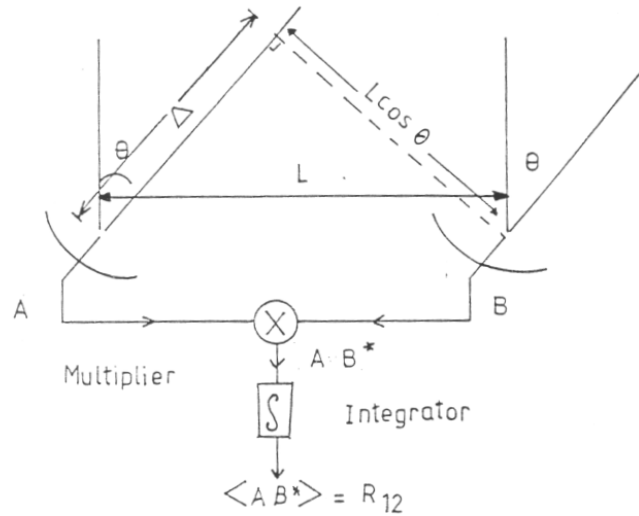


Figure 1: A simple interferometer

1.2 Simple Interferometers

The simplest radio interferometer of all consists of two aerials connected together via lengths of coaxial cable to a multiplier and integrator (figure 1). The voltages A and B from the aerials (proportional to the electric field at each aerial) are multiplied giving AB^* at the output. The AB^* term when averaged over several radio frequency cycles in the integrator is proportional to the cross - correlation R_{12} of the electric field received by the two aerials. The multiplier and integrator (and other electronics) are collectively called the correlator for this reason.

If from aerial 1 we have a signal $A = E_1 e^{i\omega t}$ and from aerial 2 we have $B = E_2 e^{i(\omega t - k\Delta)}$ where ω is the angular frequency, k the wavenumber and the signal entering aerial 2 is delayed by passing through a path length Δ . The output of the multiplier is

$$AB^* = E_1 E_2^* e^{ik\Delta} \quad (1)$$

where $\Delta = L \sin(\theta)$. The real part of this is thus a cosine wave as a function of θ (see figure 2) Note that the output of the interferometer is complex, in fact in-phase and quadrature multiplications are usually made so that amplitude and a phase can be recovered; and that the output is a function of the path delay Δ/c .

We can imagine a polar diagram of the output drawn as the angle θ between the normal baseline and the source varies. This is the fringe pattern on the sky, radio interferometry is all about finding fringes. Fringe maxima occur when $\phi = 2n\pi$ so they are spaced by λ/L in $\sin(\theta)$.

1.3 Response to an Extended Source

The interferometer output, proportional to the cross-correlation function of the electric field, can be converted to a fringe amplitude measured in Jy by multiplying by $\sqrt{S_1 S_2}$ when S_1 and S_2 are the equivalent noise temperatures of the telescopes 1 and 2 expressed in Jy (see lectures on calibration). For a point source R_{12} has a constant amplitude proportional to the flux density of the source.

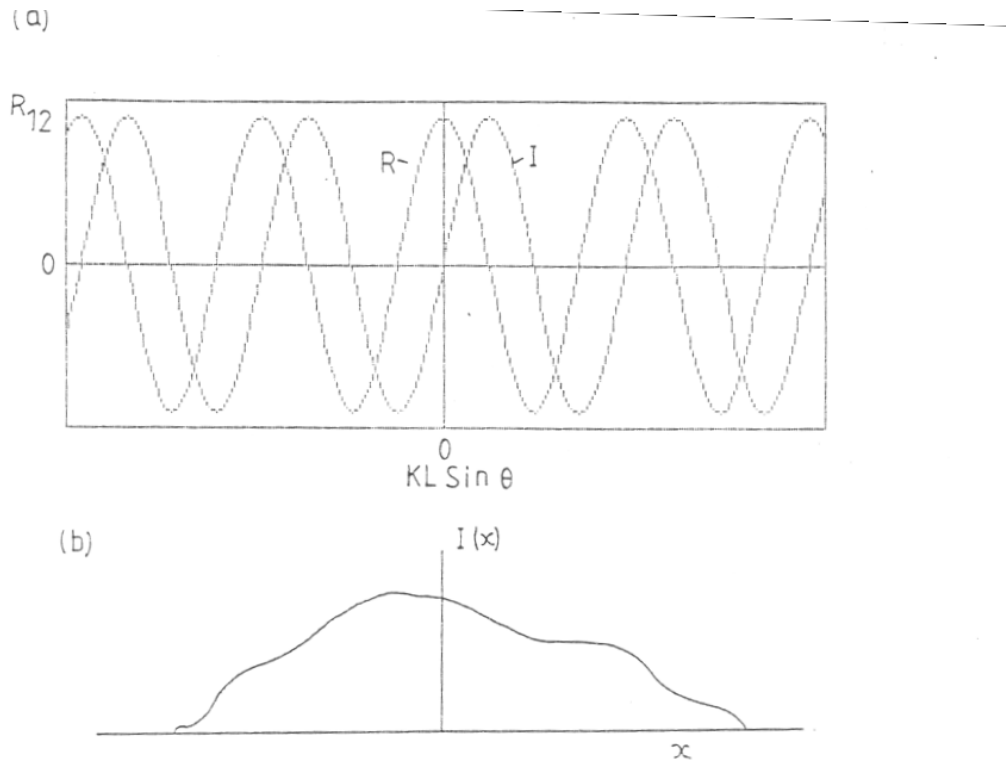


Figure 2: a) Fringe pattern of an interferometer, b) an extended source

If we imagine fringes drawn on the sky when observing an extended source then some parts of the source will give rise to a positive output while others will give a negative output (figure 2). Thus there will be some degree of cancellation in the total signal and the output signal will be reduced compared to that obtained from a source of the same total flux density. We can define a fringe visibility V as the measured fringe amplitude divided by the fringe amplitude the source would have if it were a point. V is always ≤ 1 . In the early days of interferometry visibilities were the things to measure, and visibilities from simple model brightness distributions were compared with measured data. However there is a fundamental relationship between the sky brightness distribution and the cross correlation function R_{12} which enables the sky brightness to be found directly rather than by model fitting.

Consider a sky brightness distribution (1-dimensional for now) $I(x)$ where x is the displacement in angle from the field centre, *i. e.* $x = 0$ corresponds to the angle θ to the normal with the field centre at θ (figure 2). A signal from a point x has power $I(x)dx$. Now our fringes are spread over the source, so the output of the interferometer is the sum of all the contributions, *i. e.*

$$R_{12} = \int I(x)e^{ikL\sin(\theta+x)} dx \quad (2)$$

since the contribution from x is proportional to the intensity $I(x)$, and the integral extends over the whole source (in principle the whole sky). Now for small x , $\sin(\theta + x) = \sin(\theta) + x \cos(\theta)$ and we can separate the term in $\sin(\theta)$,

$$R_{12} = e^{ikL\sin(\theta)} \int I(x)e^{ikL\cos(\theta)x} dx \quad (3)$$

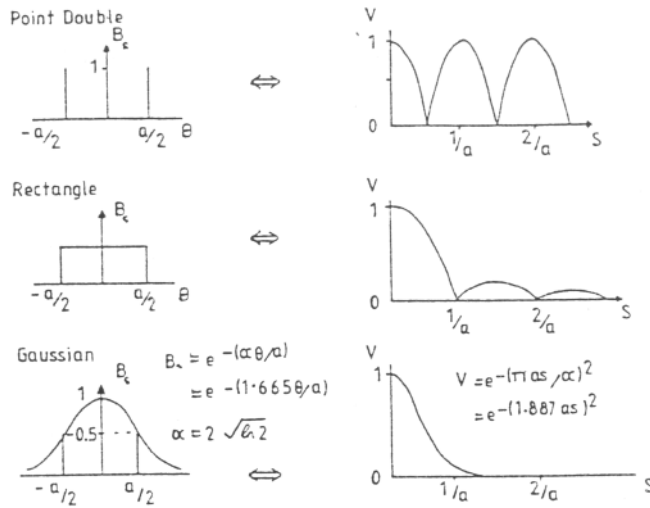


Figure 3: Response to extended sources

The term $e^{ikL\sin(\theta)}$ represents the effects due to the path delay. It is normally compensated in the correlator *via* cables or digitally to allow for a finite bandwidth *i.e.* to get the white light fringe (see section 1.4 and the appendix). The term can therefore be removed in our discussion. We can write $kL\cos(\theta) = 2\pi s$. s is a spatial frequency and is normally measured in wavelengths. The interferometer output then becomes:

$$R_{12} = \int I(x)e^{2\pi s x} dx \quad (4)$$

This is a Fourier Transform, obtained by superimposing waves from the source multiplied by a sine function so the fringe visibility can be found for any given brightness distribution *e.g.* figure 3. R_{12} is in general complex. This relationship was first discovered in the 1930's in optics and is called the van-Cittert Zernicke theorem and is valid for partially coherent, sources of radiation. More general proofs are given in Born and Wolf (1959) and in Thompson *et al.* (1987).

An interferometer at a given baseline s measures one Fourier component of the source, corresponding to that baseline. If the phase as well as fringe amplitude can be found for a number of baselines then we may be able to invert the transform and find the sky brightness distribution. *i. e.*

$$I(x) = \int_{-\infty}^{\infty} R_{12}(s)e^{-2\pi i s x} ds \quad (5)$$

If the number of spacings is such as to cover all baselines out to some maximum then we have synthesised a fully filled aperture. This process is not unexpectedly called aperture synthesis and was first applied to radio astronomy by Martin Ryle and his group.

Usually and especially in VLBI, we have a limited number of baselines and so the aperture is only partially filled. This gives rise to a limited resolution and also side lobes to the point source response.

1.4 Tracking Interferometers

So far we have not considered a fundamental fact of life: aerials or radio telescopes as we should now call them remain fixed on the ground and the sky appears to rotate above our heads. Thus the angle θ changes with time for a given source in the sky. The path delay $\Delta = L \sin(\theta)$ will change with time and source will appear to move through the fringes on the sky. Thus the output of the interferometer will be a sine wave at a frequency corresponding to the rotation rate of the Earth divided by the fringe angular spacing *i. e.*

$$\text{fringe frequency } F = (2\pi/86400)L'/\lambda$$

where $L' = L \cos(\theta)$ is the length of the baseline projected perpendicular to the source direction.

This frequency can be high (100's of Hz in VLBI) compared with the reciprocal of the averaging time typically used in a correlator (seconds) so the fringes would be smoothed out completely. An interferometer which is designed to track a source for several hours therefore needs to take this into account and fringe stop by phase rotating the input signals to the interferometer. Use of a finite bandwidth also means that the path lengths should be equal on both sides and so some device, the tracking delay, has to be incorporated in order to compensate for varying Δ . This can be achieved by switching in lengths of cable for connected element, interferometers. Early Jodrell Bank radio linked interferometers used ultrasonic transducers in a bath of mercury. MERLIN, VLBI and other modern connected element systems use electronic means. These devices are shown schematically in figure 4.

If we could make a tracking delay that would work at the incoming radio frequency signal then the geometric path compensation would work in delay and phase and so there would be no need for the phase rotator. In practice, the incoming signals are always mixed down to some convenient intermediate frequency, where the tracking delay can operate. We therefore need phase rotators to allow for the fact that the tracking delay is not operating at the same centre frequency as the geometric delay.

It is important to understand what is meant by the phase of the output signal from an interferometer. The output, signal is described by two numbers which vary as a function of baseline length. These are the amplitude and phase of the fringes in the case of an interferometer without phase rotators. They are measured by means of in phase and quadrature multipliers in most instruments. In the case of an instrument with phase rotation the phase that comes out corresponds to the difference in the phase of the signal produced by the source and that calculated by the computer doing the phase rotation. Both of these depend on the geometry of the interferometer and will vary with hour angle in a tracking interferometer (see section 2). In the ideal case with no phase errors (due to noise, atmospheric variations, or position and baseline errors), then a point source at the field centre will give a constant output signal at zero phase. A point source offset from the

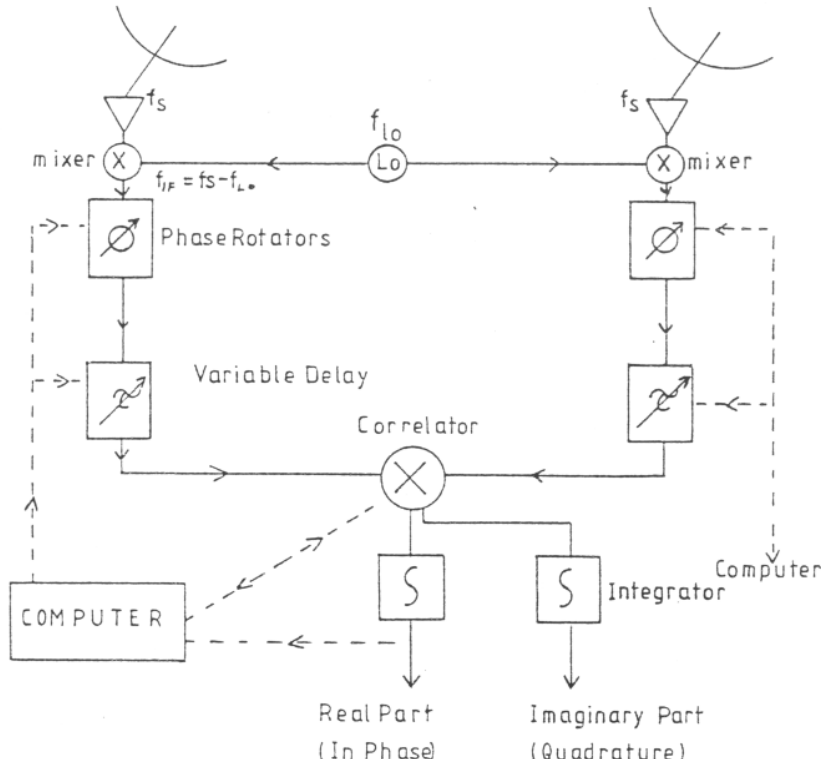


Figure 4: A long baseline interferometer

field centre will give a sine wave of constant amplitude, a frequency which depends on the magnitude of the offset and a phase which depends on the direction of the offset. In practice there are always phase errors but these can be at least partially corrected by calibration.

2 Geometrical Effects

2.1 Geometry of Earth Rotation

Use of a tracking interferometer not only enables longer observations of a source to be made, but also adds to the information available on the source structure since the projected baseline also changes as the Earth rotates. Consider the position of a telescope on the surface of the Earth as a vector to the Earth's centre. A rectangular set of coordinates in meters with the N pole in the z direction and the Greenwich meridian giving the x direction is commonly used.

Figure 5 shows a 2 telescope interferometer with a baseline vector $B = T_1 - T_2$ where $|B| = L$ the baseline length and S is a unit vector in the source direction. The path delay is $B \cdot S$ and the projected baseline seen from the source has a magnitude $|B \wedge S|$ i. e. $|B| \sin(\theta) = |b|$. From figure 5

$$b = V - (B \cdot S)S \tag{6}$$

$$b = S \wedge (B \wedge S)$$

This can be decomposed into a set of components u, v, w where w is in the source direction (strictly the centre of the field of view) u in the E-W and v in the N-S

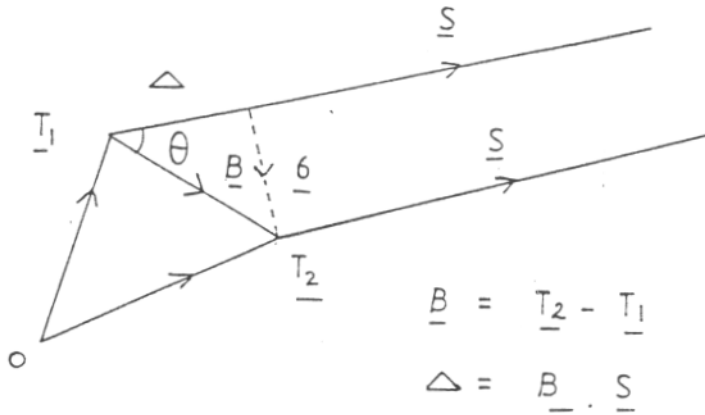


Figure 5: Two telescopes on the Earth

directions. (u, v, w) are usually measured in wavelengths for convenience. For small fields of view and E-W interferometers the w term can be neglected and we can concentrate on the projected baseline in a direction perpendicular to that of the source. (u, v, w) are spatial frequencies.

We need to resort to spherical trigonometry to find the values for a source at a given hour angle H and declination D . In matrix form the answer is

$$\begin{pmatrix} u \\ v \\ w \end{pmatrix} = \begin{pmatrix} \sin(H) & \cos(H) & 0 \\ -\sin(D)\cos(H) & \sin(D)\sin(H) & \cos(D) \\ \cos(D)\cos(H) & -\cos(D)\sin(H) & \sin(D) \end{pmatrix} \begin{pmatrix} B_x \\ B_y \\ B_z \end{pmatrix}$$

where the baseline lengths have been divided by the wavelength.

An earlier method used the concept of baseline hour angle h and declination d *i. e.* the intersection on the sky of a line drawn between the two telescopes. We can then use spherical trigonometry to derive the so called 'Interferometer Phase Equation' which tells us the phase difference Φ between the two signals in a two element interferometer. Expressions for the E-W and N-S components of the baseline can also be found (Rowson 1963). The phase equation is

$$\Phi = \frac{2\pi L}{\lambda} \{(\sin(d) \sin(D) + \cos(d) \cos(D) \cos(H - h))\} \quad (7)$$

where h, d are the hour angle and declination of the point, w here the baseline projects on the sky.

2.2 The u, v Plane

The E-W and N-S components of the projected baseline are:

$$u = \frac{L}{\lambda} \cos(d) \sin(H - h) \quad (8)$$

$$v = \frac{L}{\lambda} \{\sin(d) \cos(D) - \sin(D) \cos(d) \cos(H - h)\} \quad (9)$$

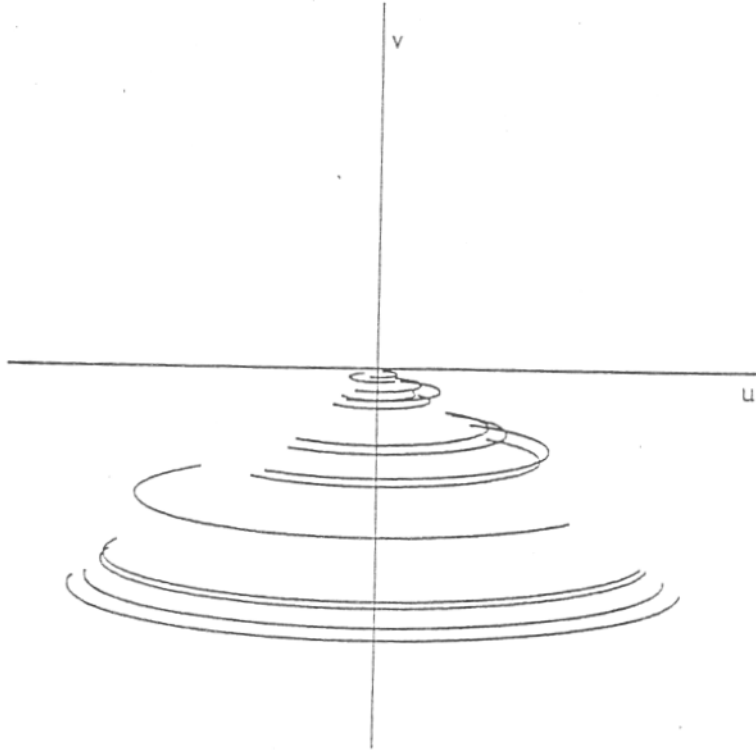


Figure 6: Variation of u, v with hour angle - the resolution plane for the MERLIN array with source at 10° declination

where u and v are measured in wavelengths. The locus of these as hour angle varies is an ellipse on the u, v plane with centre $(0, L \sin(d) \cos(D))$, semi-major axis $L \cos(d)$ and semi-minor axis $L \cos(d) \sin(D)$ as in figure 6.

The u, v plane, or 'resolution plane' is of great importance. Each pair of telescopes will give an ellipse on the u, v plane by tracking a radio source, though some part of the ellipse will be missing due to the source having set below the horizon or due to hour angle limitations of the telescopes. N telescopes in an array will give $N(N - 1)/2$ baselines and hence $N(N - 1)/2$ tracks in the u, v plane. Thus the data are sampled by a set of partial ellipses, with a data point taken every integration period. The u, v plane for a relatively simple source structure is shown in figure 7 and it is important that the relevant variations in fringe visibility are fully sampled

Since the quality of the image that can be obtained by Fourier transformation depends on the amount of u, v plane data available, most arrays of telescopes are arranged to sample the u, v plane in an optimum manner. There is a general rule that the more telescopes in an array the better the maps will be.

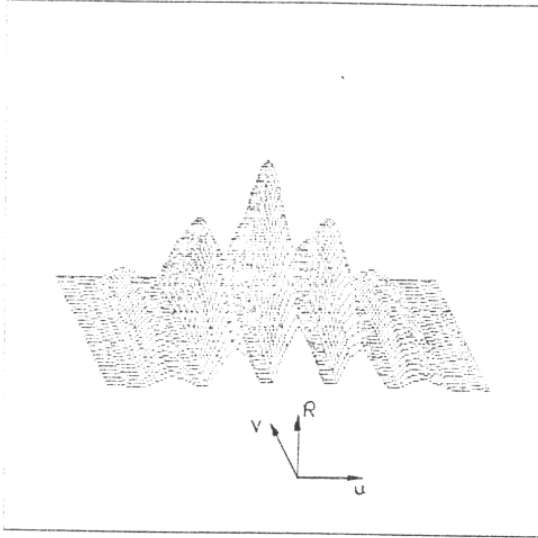


Figure 7: Visibility in (u, v) co-ordinates of a source consisting of two elliptical Gaussian components.

3 Image formation in Interferometry

Our tracking interferometer gives us amplitude and phase information corresponding to the u , v , w value at a given instant of time. u , v , w must not vary significantly during the integration time otherwise information will be lost. This set of numbers tells us about one Fourier component of the source brightness distribution, as shown by the van-Cittert Zernicke theorem. Thus the correlator output (which we have seen to be proportional to the cross correlation of the electric field at the telescopes) is given by the Fourier transform of the sky brightness viz:

$$R(u, v, w) = \int_{-\infty}^{\infty} \int_{-\infty}^{\infty} \frac{B_s(x, y)}{\sqrt{1 - x^2 - y^2}} e^{2\pi i (ux + vy + w(\sqrt{1 - x^2 - y^2} - 1))} dx dy \quad (10)$$

where (x, y) are a rectangular coordinate set drawn on the sky with origin at the field centre and x direction to the east. We have assumed that R has been calibrated and scaled so that its units are in Jansky thus ensuring that the units of the sky brightness B_s are in Jansky per beam area and we have dropped the subscripts. In terms of normal celestial coordinates $x = -\Delta(\text{RA})\cos(D)$ and $y = \Delta(D)$ where $\Delta(\text{RA})$ and $\Delta(D)$ are the offsets in Right Ascension and Declination.

We can see that the w term causes problems in that we no longer have a simple transform. It turns out that w can be neglected in most cases of interest (see appendix) and so a much simpler expression results

$$R(u, v) = \int_{-\infty}^{\infty} \int_{-\infty}^{\infty} B_s(x, y) e^{2\pi i(ux+vy)} dx dy \quad (11)$$

since x^2 and y^2 are small compared with 1. This can be inverted

$$B_s(x, y) = \int_{-\infty}^{\infty} \int_{-\infty}^{\infty} R(u, v) e^{-2\pi i(ux+vy)} dx dy \quad (12)$$

This is a simple extension to 2 dimensions of the argument used in section 1. So if we have amplitude and phase information over the whole of the u, v plane *i.e.* from lots of interferometers in an array, then the sky brightness can be found. Note that the sky brightness B_s is real, so that R is Hermitian *i.e.*

$$R(u, v) = R^*(-u, -v) \quad (13)$$

so we have twice as much u, v coverage as we thought! Another way of thinking about this is that we have information from a baseline extending from telescope 1 to telescope 2 and information from a baseline from telescope 2 to telescope 1. They are the same but for the phase reversed.

Of course we would need an infinite number of telescopes to 'fill the u, v plane' so in practice a discrete transform is made where to first order the maximum baseline length L_m gives us the resolution λ/L_m , and the gaps in the u, v coverage give rise to sidelobes in the synthesised beam. The beam of the synthesised telescope is given by the Fourier transform of a set of unity values at each u, v point, and it is the same as the point source response. This is called the *Dirty Beam*.

Thus an estimate of the true sky brightness B_e can be made by using a direct Fourier transform of $R(u, v)$ *i.e.*

$$B_e(x, y) = \sum_{j=1}^M R(u_j, v_j) e^{-2\pi i(u_j x + v_j y)} \quad (14)$$

for each pixel in our map and where M is the number of measured u, v points. This is called the principal solution and it implicitly assumes that $R = 0$ at the points that were not measured. Putting $R = 1$ in this equation gives us the Dirty Beam.

Directly performing the Fourier transform in this way is computationally expensive (M can be several million!) and most analysis packages use the Cooley-Tukey Fast Fourier transform (FFT). This requires the data to be interpolated on to a regular grid of $2^n \times 2^n$ data points, and the programs use various degrees of sophistication in the way that the interpolation is done. Typically maps which are 512 by 512 pixels are made from a million u, v data points.

The grid spacing is chosen to fully sample the synthesised beam *i.e.* ~ 3 pixels per FWHM of the beam. The FFT can be performed quickly, giving us an estimate of the sky brightness which is called the *Dirty Map*. This map is the *convolution* of the true sky brightness with

the Dirt Beam and so has nasty sidelobes and other confusing features. Nearly all the images produced by the VLA and MERLIN have been *CLEAN'ed*, a process of de-convolution whereby the map is decomposed into a set of spikes or delta functions. These are then convolved with an ideal beam with no side lobes, usually an elliptical gaussian, to give the final image.

4 Concluding Remarks

We have seen how simple interferometers work and learnt that the output of an interferometer is the Fourier transform of the sky brightness distribution. The spatial frequencies over which the data are measured vary with hour angle as the earth rotates, forming an ellipse in the resolution or u, v plane. These data are Fourier inverted to give an estimate of the sky brightness distribution, and is from this that our astrophysics will eventually be derived.

Further effects due to finite bandwidth, 3-D geometry and subsequent limitations to field of view of an interferometer are considered in the appendix. More details can be found in Perley *et al.* 1989, Thompson *et al.* 1986 and Felli and Spencer 1989, the latter two references being particularly relevant to VLBI.

References

- Born, M. and Wolf, E., 1959, *Principles of Optics* Pergamon, London, and later editions.
Bracewell, R.N., 1965, *The Fourier Transform and its Applications*, McGraw Hill, New York.
Felli, M. and Spencer, R.E., 1989, *Very Long Baseline Interferometry Techniques and Applications*, Kluwer, Dordrecht.
Perley, R.A., Schwab, F.R. and Bridle, A.H., 1989, *Synthesis Imaging In Radio Astronomy*, ASP, San Francisco.
Rowson, B. 1963, *Mon. Not. R. astr. Soc.* 125, 177
Thompson, A.R., Moran, J.M., and Swenson, G.W. 1986. *Interferometry and Synthesis in Radio Astronomy*, Wiley.

APPENDIX

Limitations to the field of view of an Interferometer

A number of different effects limit the maximum size of the region to be mapped (field of view) by an interferometer, in addition to the obvious restrictions of computer power on the number of pixels that can be handled. They are as follows:

A.1 Primary Beamwidth

The primary beams of the telescopes used will limit the field of view. The limit normally chosen is λ/D where D is the diameter of the largest telescope. Some extra care has to be taken when synthesis arrays like the Westerbork Telescope are used in VLBI.

A.2 Effects of a finite bandwidth

So far we have only considered monochromatic signals. In practice the receivers have a finite bandwidth, indeed large bandwidths are required to get high sensitivity on continuum sources. This means that the geometric path delay is different for the different frequencies within the band and it may lead to signals being out of phase. Extra path delay has to be introduced to ensure that the delays on each side of the interferometer are equal, i.e., the 'white light' fringe becomes detectable. This can be done by switching in extra cables for a connected element interferometer or by electronic memory devices in a digital system. The path delay, $\phi\lambda/(2\pi c)$ can amount to several milliseconds in a VLBI system.

Multiplication of the two incoming signals in a two element interferometer leads to various cross products when the signals have finite bandwidths even when we have ensured the same path delay at the band centre through each arm. The output of the correlator after integration for a time T can be written as

$$R(\tau) = \lim_{T \rightarrow \infty} \frac{1}{2T} \int_{-T}^T v_1(t)v_2(t - \tau)dt \quad (15)$$

where T is the differential delay between the two signals. In practice T cannot go to infinity, it has to be less than the fringe period. However the important thing is that T is much greater than the reciprocal bandwidth so that many cycles are averaged. Usually T is a second or more.

The signals from each telescope have a power spectrum which results from the intrinsic nature of the incoming radiation (assumed to be flat over the band for continuum radiation) and the receiver gain characteristics. We will suppose that the arms of the interferometer have identical voltage gains $H(\nu)$ as a function of frequency (figure 8).

Now the Fourier transform of the correlator output is

$$|H(\nu)|^2 = \int_{-\infty}^{\infty} R(\tau)e^{-2\pi\nu\tau} d\tau \quad (16)$$

where we have used the Wiener Isinchine theorem which states that the power spectrum of a signal is given by the Fourier transform of the auto correlation of the

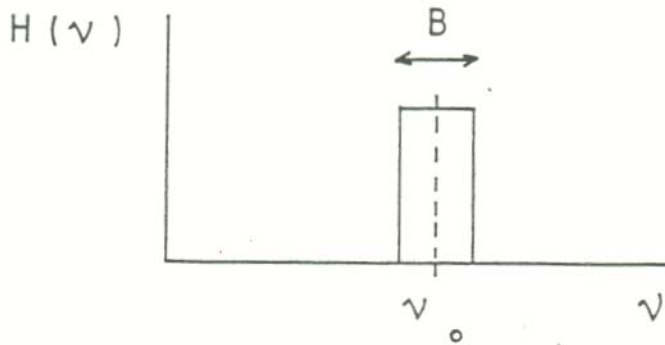


Figure 8: Receiver response

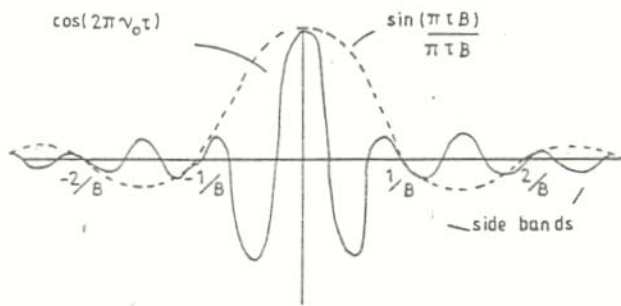


Figure 9: Correlator output as a function of delay

signal. If we have a rectangular passband centred at ν_0 and bandwidth B then

$$|H(\nu)|^2 = \Pi * \delta(\nu - \nu_0) \quad (17)$$

where Π is a top hat function, δ a delta function and $*$ denotes convolution. It therefore follows that the correlator output becomes

$$R(\tau) = a \frac{\sin(\pi\tau B)}{\pi\tau B} e^{2\pi i\nu_0\tau} \quad (18)$$

This is sketched in figure 9 and is variously known as the delay pattern, bandwidth pattern or fringe washing function. Note that the pattern has sidebands due to the sinc function ($\sin(x)/x$). It has been known for interferometers to be set up erroneously on a sideband of the delay pattern by using the wrong fixed delay! In practice the receiver bandpasses are not rectangular but have a smoother response. This usually results in sidebands of lower relative amplitude. Further the two sides of an interferometer may not have an identical gain characteristic. This can result in a loss of sensitivity and a curious looking delay pattern. The closure amplitudes are also effected (see later lectures) and therefore some effort should be made to provide matched receivers.

Notice that a source situated away from the centre of the field of view (for which the phase and delay calculations have been made for a tracking interferometer) will have a different delay T . The interferometer response on this source will therefore be reduced relative to that for a source at the field centre. The width of the delay pattern is roughly $1/B$, so a source more than $c/(L.B)$ away from the field centre will be reduced in response. For 100 km baseline and 16 Mhz bandwidth the maximum instantaneous field of view is about 38 arc sec.

A.3 Integration Time

The basic integration time used by the correlator will limit the field of view if the u, v values change significantly in this time. Averaging the correlator output for a time $2T$ gives

$$\frac{1}{2T} \int_{-T}^T R(u, v) dt$$

and since the values of (u, v) change over the time $2T$ this can be written

$$\Pi\left(\frac{2u}{\Delta u}, \frac{2v}{\Delta v}\right) * R(u, v)$$

where Π is a 2-dimensional top hat function of widths Δu and Δv and $*$ implies convolution. Time $2T$ corresponds to a change of Δu in u and Δv in v as the Earth rotates. Inverting this gives an estimate of the true sky brightness B_s :

$$B'_s(x, y) = \text{sinc}(2x\Delta u) \text{sinc}(2y\Delta v) B_s(x, y) \quad (19)$$

In other words the measured sky brightness is restricted, with FWHM in the E-W and N-S directions given by $x_{max} = \pm\pi/(2\Delta u)$ and $y_{max} = \pm\pi/(2\Delta v)$. For example a baseline 100,000 wavelengths long has a lobe size of 2 arc sec and a field of view of 6 arc min FWHM.

A.4 The w term or the effects of non planar geometry. In vector form equation (10) can be written

$$R = \int B_s e^{2\pi i \mathbf{B} \cdot (\mathbf{S} + \boldsymbol{\sigma})} d\boldsymbol{\sigma} \quad (20)$$

where $\boldsymbol{\sigma}$ is a small displacement from the field centre at \mathbf{S} . Now the projected baseline as seen from the source is

$$\mathbf{b} = \mathbf{B} - (\mathbf{B} \cdot \mathbf{S}) \mathbf{S} \quad (21)$$

(equation 6), but the transform above uses

$$\mathbf{B} \cdot (\mathbf{S} + \boldsymbol{\sigma}) = \mathbf{B} \cdot \mathbf{S} + \mathbf{B} \cdot \boldsymbol{\sigma} = \mathbf{B} \cdot \mathbf{S} + \mathbf{b} \cdot \boldsymbol{\sigma} + (\mathbf{B} \cdot \mathbf{S}) (\mathbf{S} \cdot \boldsymbol{\sigma}) \quad (22)$$

The projected baseline \mathbf{b} is composed into E-W and N-S components u and v . This leaves us with the 3rd term in equation (22) which is only zero if $\mathbf{S} \cdot \boldsymbol{\sigma}$ is zero i.e. \mathbf{S} perpendicular to $\boldsymbol{\sigma}$ (see figure 10).

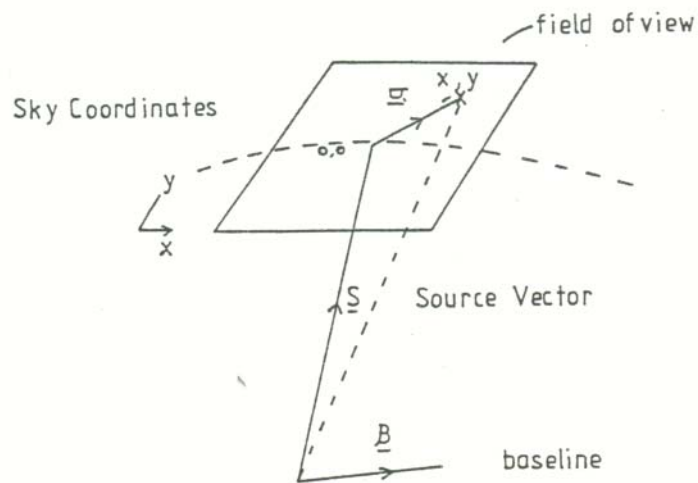


Figure 10: Non planar geometry

Consideration of the true geometry leads to the zv terms. For an E W interferometer like the Cambridge 5 km or the Westerbork array w is zero. We can estimate the error caused by its neglect as follows: if θ_B is the FWHM beamwidth of the synthesised beam (λ/L) and θ_F the field size to mapped then the maximum phase error at the edge of the map will be

$$\sim \frac{\pi \theta_F^2}{4 \theta_B}$$

If this is less than 0.2 radian then $\theta_F < \sqrt{0.25} \theta_B$ e.g. less than 22 arcsec for a 10 milliarcsec beam.

Which of the above limitations dominates depends on the instrument, bandwidth etc. used and should be worked out before observations of an extended source are made.